

New grids of ATLAS9 atmospheres I: Influence of convection treatments on model structure and on observable quantities

U. Heiter^{1,2}, F. Kupka¹, C. van 't Veer-Menneret³, C. Barban^{3,4}, W.W. Weiss¹, M.-J. Goupil³, W. Schmidt^{1,5}, D. Katz³ and R. Garrido⁶

¹ Institut für Astronomie, Universität Wien, Türkenschanzstrasse 17, A-1180 Vienna, Austria; email: last-name@astro.univie.ac.at

² Department of Astronomy, Case Western Reserve University, 10900 Euclid Avenue, Cleveland, OH 44106-7215, USA; email: ulrike@fafnir.astr.cwru.edu

³ Observatoire de Paris-Meudon, 5, Place Jules Janssen, F-92195 Meudon Cedex, France; email: Claude.VantVeer@obspm.fr, Caroline.Barban@obspm.fr, MarieJo.Goupil@obspm.fr, David.Katz@obspm.fr

⁴ National Solar Observatory, 950 N. Cherry Ave., Tucson, AZ 85719, USA; email: barban@noao.edu

⁵ Max-Planck-Institut für Astrophysik, Karl-Schwarzschild-Str. 1, D-85741 Garching, Germany; email: wschmidt@mpa-garching.mpg.de

⁶ Instituto de Astrofísica de Andalucía, C.S.I.C., Apdo. 3004, 18080, Granada, Spain; email: garrido@iaa.es

Received ; accepted

Abstract. We present several new sets of grids of model stellar atmospheres computed with modified versions of the ATLAS9 code. Each individual set consists of several grids of models with different metallicities ranging from $[M/H] = -2.0$ to $+1.0$ dex. The grids range from 4000 to 10000 K in T_{eff} and from 2.0 to 5.0 dex in $\log g$. The individual sets differ from each other and from previous ones essentially in the physics used for the treatment of the convective energy transport, in the higher vertical resolution of the atmospheres and in a finer grid in the $(T_{\text{eff}}, \log g)$ plane. These improvements enable the computation of derivatives of color indices accurate enough for pulsation mode identification. In addition, we show that the chosen vertical resolution is necessary and sufficient for the purpose of stellar interior modelling. To explain the physical differences between the model grids we provide a description of the currently available modifications of ATLAS9 according to their treatment of convection. Our critical analysis of the dependence of the atmospheric structure and observable quantities on convection treatment, vertical resolution and metallicity reveals that spectroscopic and photometric observations are best represented when using an inefficient convection treatment. This conclusion holds whatever convection formulation investigated here is used, i.e. MLT ($\alpha = 0.5$), CM and CGM are equivalent. We also find that changing the convection treatment can lead to a change in the effective temperature estimated from Strömgren color indices from 200 to 400 K.

Key words. stars: stellar atmospheres – stars: fundamental parameters – stars: δ Scuti stars – physical data and processes: convection

1. Introduction

Convective transport of energy in a stellar atmosphere is one of the most complex astrophysical problems. Many of the approximations usually admitted for the stellar interior, such as diffusive radiative transfer, are no longer valid. Moreover, throughout most of a convective stellar atmosphere radiative losses are large enough to make convection less efficient in transporting energy than radiation. Only stars which have a surface convection zone (CZ) extending deep into the stellar envelope can maintain efficient convective energy transfer near the bottom of their

atmosphere. On the other hand, inefficient convection appears in all stars near the boundary of a convection zone close to locally stable regions. The modelling of inefficient convection requires a detailed knowledge about the effect of radiative gains and losses on the fluid flow. The situation is particularly complex for stars which are cool enough to develop a granulation pattern, such as the sun. In this case, at identical geometrical depths, vastly different physical conditions may be encountered depending on whether upflow in a granule or downflow in an intergranular lane is considered. The former may be optically thick while the latter is already optically thin, a consequence of the extreme temperature sensitivity of the dominant

opacity source in the solar photosphere, the H^- ion (cf. also Stein & Nordlund 1998).

Currently, only very simple convection models are available for routine computation of extended grids of model atmospheres, while detailed numerical simulations are still unaffordable for applications that require the calculation of many thousands of individual model atmospheres over the HR diagram.

Our intention here is first to review the convection models which are available for use together with the popular ATLAS9 model atmosphere code by Kurucz (1993, 1998) (see also Castelli et al. 1997). We provide an overview on what is known about the effects of the different convection treatments on model atmosphere structure and consequently on observable quantities.

The second purpose of the present paper is to determine to what extent the precision of fundamental parameters derived from the observed stellar spectrum, i.e. T_{eff} , gravity and metallicity depend on the model atmosphere.

Another objective is to obtain very accurate colors and more importantly very accurate derivatives of colors, color indices and limb darkening coefficients. These quantities are needed in the procedure of pulsation mode identification which is the first and a crucial step in any seismological study. Indeed probing the stellar interior of a pulsating star requires the knowledge of the resonant cavity within which each mode propagates, i.e. the physical nature of the pulsation mode associated with each observed oscillation frequency. One such procedure is based on the computation of oscillation amplitude ratios and phase differences which in turn depend on the variation of the colors with effective temperature and gravity. The results of this application of the model atmosphere grids will be presented in the next papers of this series (Barban et al. 2002; Garrido et al. 2002). Finally, due to their enhanced resolution the new model grids are also useful to improve the outer boundary conditions of stellar structure calculations (Montalbán et al. 2001; D'Antona et al. 2002).

These goals are part of a program performed in the framework of preparing the COROT space mission (see COROT web site). To achieve these purposes, we have used the ATLAS9 code in several versions modified for the convection zone treatment to compute new grids of model atmospheres, corresponding fluxes, surface intensities, *uvby* colors, synthetic spectra for some representative lines, and compared them with relevant observations. We have three versions of the ATLAS9 code at our disposal:

1. The original version from CDROM13 of Kurucz (Kurucz 1993) in which the convection zone is treated using mixing length theory (MLT). While ATLAS versions from 5 to 8 remained basically close to the formulations given in Böhm-Vitense (1958) and in Cox & Giuli (1968), some improvements were added in ATLAS9 (cf. Castelli et al. 1997). In Sect. 2 we discuss the reasons for our specific selection among these improvements.
2. The other two versions were provided by one of the authors (FK) who modified the code to include turbulent convection models from Canuto & Mazzitelli (1991, CM), and from Canuto, Goldman, & Mazzitelli (1996, CGM).

Each convection model has been extensively used in the model atmosphere grid computations which we describe below. All the convection models are of local type and thus require the prescription of a characteristic length scale. Formally, it is possible to interchange the different length scales associated with the convection models. The motivation for doing so and a particular example will be discussed in the next paper of this series (Kupka et al. 2002).

This paper is organized as follows. In Sect. 2 we review previous works about the effect of the model structure on theoretical photometric colors and justify the need for new grids of model atmospheres. In Sect. 3 we describe the specific different convection treatments used and discuss their physical content.

In Sect. 4 we give details of the grid computations. In Sect. 5 we set out and comment the role of the convection treatments and convection parameters on the model structure, as well as its dependence on effective temperature, surface gravity, and metallicity. Finally, we discuss the consequences on observable quantities such as Balmer line profiles, flux distributions, and colors.

2. A need for new grids

The original grids of model atmospheres and colors based on the ATLAS9 code were published by Kurucz (1993). They were computed using the classical mixing length theory. Kurucz chose and fixed the mixing length parameter α , i.e. the ratio l/H_p of convective scale length l and local pressure scale height H_p , to be 1.25. He also used a prescription for overshooting at the top of the convection zone (cf. also Sect. 3) to achieve a better match between computed and observed solar fluxes for the range of α considered. The parameters obtained from the comparison with solar data were used for the entire grids published in Kurucz (1993). These grids have now been superseded by a new set with a slightly modified prescription of the overshooting treatment (for details see Castelli et al. 1997). More recently, they have also become available in electronic form (Kurucz 1998).

Castelli et al. (1997) compared Johnson colors and the $(b-y)$ and c indices from the Strömgren system with colors from grids of model atmospheres based on MLT with and without the overshooting prescription, and with an identical choice for the mixing length. Considering different methods of determining T_{eff} they concluded that models without the overshooting treatment yield more consistent results, while for the solar case a model with overshooting was favored. As a consequence of this study, new grids of models, fluxes and colors were computed by Castelli without any overshooting for several metallicities and different microturbulent velocities. They are available at the

Kurucz website (“NOVER” grids). Castelli (1999) analysed synthetic Johnson UBV colors from these model atmosphere grids, all based on MLT with $\alpha = 1.25$. She analysed the effect of metallicity and microturbulent velocity and concluded that the indices are affected by both the convection treatment and the amount of line blanketing. This has to be considered in parameter determinations for stars with unknown metallicity.

Künzli et al. (1997) have used the revised version of model atmosphere grids of Kurucz (1998) to provide a new calibration of Geneva photometry for B to G type stars. Comparing their photometrically determined T_{eff} and $\log g$ with evolutionary tracks for the Hyades they noticed a systematic trend in T_{eff} below 7000 K and a rather pronounced “bump” in $\log g$ located in the same region. Both results were considered to indicate shortcomings in the model atmospheres used for the computations of the synthetic color indices.

Smalley & Kupka (1997, SK) were the first to study the role of different convection treatments implemented in the ATLAS9 code of Kurucz (1993, 1998) for the synthetic *uvby* colors. They compared observed color indices with synthetic ones computed using two versions of ATLAS9: the original version of Kurucz (1993) based on MLT treatment of convection, with and without the overshooting option, and another version modified to employ the convection model of Canuto & Mazzitelli (1991, 1992), known as the CM model and described in Sect. 3. For the MLT they prove that models built with overshooting at the top of the convection zone, as illustrated in Castelli et al. (1997), are discrepant with the observed color indices. This confirmed similar conclusions drawn by van ’t Veer-Menneret & Megessier (1996, hereafter VM) for the case of Balmer line profiles. SK also showed that the CM models give results generally superior to those obtained with MLT using $\alpha = 1.25$, because they are in better overall agreement with the observed indices $(b - y)_0$ and c_0 . The metallicity index m_0 was found to be the most discrepant one with observations, the CM models remaining in good agreement only for stars with T_{eff} larger than 7000 K, but clearly discrepant for solar type stars. A peculiar feature in the gravity sensitive c_0 -index for T_{eff} around 7000 K was found to be present in colors predicted using any of the convection models investigated, similar to the results found by Künzli et al. (1997) for MLT model atmospheres for the Geneva photometric system.

A similar investigation to the one of SK for the Strömgren photometric system was done later by Schmidt (1999), but for the Geneva system. Moreover, he extended it to the CGM convection model which had meanwhile been implemented into the ATLAS9 code (see Sect. 3). His main conclusion, similar to the one of SK, can be summarized as follows: *synthetic color indices are more sensitive to the scale length used than to the particular convection model*. For instance, a value of $\alpha = 1.25$ yields differences in the colors in comparison with models where $\alpha = 0.5$ which are much larger than the difference among CM and CGM models as well as MLT models with $\alpha = 0.5$. He

concluded that a value of $\alpha = 1.25$ does not allow reproducing the observed photometric colors of late A and F stars. However, discrepancies were also found for the other convection treatments he had studied, in agreement with the results of SK on the *uvby* colors.

Heiter et al. (1998) investigated the temperature structure and observed quantities calculated with different convection models for two λ Bootis stars with $([M/H], T_{\text{eff}})$ values of $(-1, 6800 \text{ K})$ and $(-2, 7800 \text{ K})$. They found a smaller difference between the synthetic colors and fluxes and the observations when using the CM model or MLT without overshooting compared to MLT with overshooting (α was set to 1.25 for the MLT models). For the cooler one among the two stars, the inclusion of overshooting changed the C, Ti, Cr, and Fe abundances derived from high resolution spectra by +0.1 dex. They also compared the UV fluxes of these stars with IUE and TD1 measurements and found the CM convection model to yield results in best overall agreement while the discrepancies were largest for MLT models with $\alpha = 1.25$ with overshooting.

Recently, Gardiner et al. (1999) extended the comparison of SK to the CGM model for the case of Balmer line profiles. It was found that differences between model atmospheres based on the CM or CGM convection treatment, and models based on MLT without overshooting yield rather similar results, while MLT models with overshooting are clearly different. A recommendation for a particular model was found to be possible only for distinct, limited regions in T_{eff} . Their results indicated that a more thorough study of the hydrogen line broadening mechanisms is necessary to draw more reliable conclusions on the convection model, as well as a larger number of standard stars with more accurately known fundamental parameters. For cool dwarf stars such as the sun, one source of problems in matching observed Balmer line profiles with synthetic ones has been to neglect the self-broadening (line broadening due to collisions with neutral hydrogen) in the hydrogen line profile calculations (Barklem et al. 2000). However, this effect is too weak in A and F stars to explain the extent of the discrepancies found in matching the Balmer lines H_α and H_β with some of the model atmospheres for the stars in the above mentioned works.

From these previous works we have thus drawn the following considerations for our grid computations. First, the overshooting prescription of ATLAS9 was generally found to be less successful in reproducing observations for A to G type stars, even though for solar observations the case is less settled. Thus, we have decided not to include models computed with this treatment in our grids. However, for comparison we computed individual models with overshooting (always using the correction by Castelli (1996)) for our case studies (Figs. 2, 5 and 8).

Second, it has been found that model atmospheres which predict temperature gradients closer to the radiative one, i.e. where convection is less efficient than predicted by MLT models with $\alpha > 1$, are in better overall agreement with observations. This was first noticed by Fuhrmann et al. (1993) and, quite independently, for the

case of ATLAS9 models by VM where in order to reproduce the sequence of Balmer line profiles of the sun with the same solar model they had to reduce the value of α of their MLT model atmospheres down to 0.5. Similar results were found by Fuhrmann et al. (1993), VM and van 't Veer-Menneret et al. (1998) for a large range of metallicities and stars of spectral types between A5 and G5 where Balmer lines are both strong and primarily sensitive to the temperature stratification. As shown above, this overall conclusion can also be drawn from other types of measurements such as photometry and is found to hold in particular for A type stars with T_{eff} larger than 7000 K, while results for stars with lower T_{eff} were generally more discrepant. Consequently, we have decided to base the majority of our model grid computations on convection treatments which predict less efficient convection than the previous model grids published by Kurucz (1993, 1998) and Castelli (1999).

As far as oscillation mode identification procedures are concerned, it has been demonstrated that the dependency of the colors on T_{eff} and $\log g$ is not captured smoothly enough by the standard ATLAS9 models. The effects of the non smooth behavior of the color and limb darkening coefficient derivatives are larger than the expected effect used for identifying the modes (Garrido 2000). In order to obtain smooth variations of these quantities, we have found that it is necessary to compute our model atmospheres with a higher resolution in temperature distribution with depth and built finer grids in T_{eff} and $\log g$.

3. Convection Treatment: MLT and FST versions of ATLAS9

3.1. Mixing length theory (MLT)

Model atmospheres computed with ATLAS9 are based on the classical assumptions of stationarity and horizontal homogeneity. With these restrictions only some of the properties of stellar convection can be taken into account. ATLAS9 permits to include:

1. the thermal contributions of convection to the energy flux through the atmosphere;
2. the effect of convective motions on the line opacity due to the additional Doppler broadening of spectral lines caused by turbulent velocity fluctuations on length scales smaller than the mean free optical path. This is achieved by specifying a microturbulent velocity v_{micro} (cf. Gray 1992).
3. Optionally, ATLAS9 permits to account for changes in pressure stratification due to a turbulent pressure p_{turb} .

The convective energy flux F_{conv} in the different versions of ATLAS has been computed traditionally with the classical mixing length theory (cf. Biermann 1948; Öpik 1950; Böhm-Vitense 1958; Castelli et al. 1997). Classical MLT includes radiative cooling of the fluid which is particularly important where convection is most inefficient, near

the boundary of stably stratified layers. It requires the specification of a characteristic scale length l which is prescribed to be a fraction α of the local pressure scale height,

$$H_p = \frac{P}{\rho g} = \frac{l}{\alpha}. \quad (1)$$

l is used to describe the distance which fluid elements can travel before they dissolve. It also specifies the geometrical size of the fluid elements (“bubbles”) together with a second parameter, the ratio of the fluid element volume V over its surface area A . The quantity $V/(Al)$ has been changed during upgrades of the ATLAS code (cf. Castelli 1996). The present choice results in the same convective efficiency as the original one of Böhm-Vitense (1958) if slightly smaller values of α are used, i.e. the usual choice of $\alpha = 1.25$ in the grids of Kurucz (1993, 1998) corresponds to an “ α_{BV} ” of about 1.4 for A to G type main sequence stars. A detailed summary of the modifications of MLT as used in the ATLAS code can be found in Castelli (1996), together with various numerical coefficients which we have kept unaltered.

One strong motivation to apply a more complete description of stellar turbulent convection stems from the result that low values of the scale length parameter α , e.g. 0.5, are required to fit Balmer line profiles for the sun and other cool dwarfs (Fuhrmann et al. 1993, VM), while much larger values (between 1 and 2) are necessary to reproduce their observed radii (Morel et al. 1994). Likewise, the scale length ratio has to be varied over an even larger domain ($1 < \alpha < 3$) to reproduce the red giant branch in HR diagrams of galactic open clusters and associations for stars with masses ranging from $1 M_{\odot}$ to $20 M_{\odot}$ (Stothers & Chin 1997, 1995).

3.2. Full spectrum turbulence (FST) convection models

An alternative to MLT which can address these problems was introduced by Canuto & Mazzitelli (1991, 1992) and is referred to as the CM convection model. An improved version was proposed by Canuto et al. (1996) which is known as the CGM formulation. A main intention behind both models was to improve the physical description of convection while keeping computational expenses as low as for MLT. Both models achieve this goal by providing a gradient (diffusion) approximation for the convective (enthalpy) flux:

$$F_{\text{conv}} = K_t \beta = K_{\text{rad}} T H_p^{-1} (\nabla - \nabla_{\text{ad}}) \Phi(S), \quad (2)$$

where $K_{\text{rad}} = 4acT^3/(3\kappa\rho)$ is the radiative conductivity, $\Phi = K_t/K_{\text{rad}}$ is the ratio of turbulent to radiative conductivity, and

$$\beta = - \left(\frac{dT}{dz} - \left(\frac{dT}{dz} \right)_{\text{ad}} \right) = T H_p^{-1} (\nabla - \nabla_{\text{ad}}) \quad (3)$$

is the superadiabatic gradient. The convective efficiency S is given by

$$S = \text{Ra} \cdot \text{Pr} = \frac{g\alpha_v \beta l^4}{\nu \chi} \cdot \frac{\nu}{\chi}, \quad (4)$$

Ra and Pr are Rayleigh and Prandtl numbers of the convective flow, α_v is the volume expansion coefficient, and the meaning of the other symbols is standard. We recall here that the thermometric conductivity χ is related to the radiative conductivity through $K_{\text{rad}} = c_p \rho \chi$ and that ν is the kinematic viscosity. The quantity S is a useful measure of efficiency for flows which feature a very low Pr number, as occurs in stellar convection, and for which hence the detailed dependence on ν can be neglected in parameterisations. This is possible because viscous processes act on much longer timescales than radiation ($t_\chi = l^2/\chi$) and buoyancy ($t_b = (g\alpha_v\beta)^{-1/2}$) which in turn are responsible for the energy balance in stellar atmospheres and envelopes. Thus, the convective efficiency in a star can be characterized using only $(t_\chi/t_b)^2 = S$. The latter can easily be related to an efficiency definition more common in astrophysics (Cox & Giuli 1968) that uses the quantity

$$\Gamma = \frac{1}{2} \left((1 + \Sigma)^{1/2} - 1 \right), \quad (5)$$

where

$$\Sigma = 4A^2(\nabla - \nabla_{\text{ad}}) = \frac{2}{81}S, \quad A = \frac{Q^{1/2}c_p\rho^2\kappa l^2}{12acT^3} \sqrt{\frac{g}{2H_p}}, \quad (6)$$

and in which $Q = TV^{-1}(\partial V/\partial T)_P = 1 - (\partial \ln \mu/\partial \ln T)_P$ is the variable average molecular weight. Using this notation the MLT of Böhm-Vitense (1958) can be viewed as a phenomenologically derived prescription to compute Φ which reads

$$\begin{aligned} \Phi^{\text{MLT}} &= \frac{9}{8}\Sigma^{-1} \left((1 + \Sigma)^{1/2} - 1 \right)^3 \\ &= \frac{729}{16}S^{-1} \left(\left(1 + \frac{2}{81}S\right)^{1/2} - 1 \right)^3, \end{aligned} \quad (7)$$

as mentioned by Canuto & Mazzitelli (1991) who pointed out that alternatively the MLT can be understood as a one-eddy approximation made for the spectrum $E(k)$ of turbulent kinetic energy (see also Lesieur 1990). The latter describes how the kinetic energy of the velocity field generated by convection is distributed among different spatial scales k^{-1} . Canuto (1996) has shown how MLT underestimates the convective flux in the high efficiency regime ($S \gg 1$) while it overestimates F_{conv} in the low efficiency regime ($S \ll 1$).

Both the CM and CGM convection models attempt to overcome the one-eddy approximation by using a turbulence model to compute the full spectrum $E(k)$ of a turbulent convective flow for a given S , but keep the assumption of horizontal homogeneity and the Boussinesq approximation used in MLT. Hence, they are also referred to as *full spectrum turbulence (FST)* convection models.

In the case of the CM convection model, the so-called eddy damped quasi-normal Markovian (EDQNM) model (Orszag 1977) of turbulence is used to compute $\Phi(S)$. This model provides a rather detailed treatment of the non-linear interactions in a turbulent flow, but requires the specification of a growth rate. The latter was computed

from the linear unstable convective modes. To avoid the solution of the equations of the turbulence model each time in a stellar code, the results for F_{conv} were tabulated in a dimensionless form. This was achieved by computing the quantity $\Phi(\text{Ra}, \text{Pr})$ for a large range of Ra and Pr numbers. For $\text{Pr} < 10^{-3}$ the function Φ was found to saturate. This agrees with the previous remark that S is a useful measure of convective efficiency in a star, where Pr is even orders of magnitudes lower, and it was hence sufficient to consider only the results for the lowest Pr number for a tabulation of $\Phi(S)$, or actually $\Phi(\Sigma)$, given by the EDQNM model. Canuto & Mazzitelli (1991) found that $\Phi(\Sigma)$ can be represented by the following analytical fit formula to an accuracy of better than 3%:

$$\Phi^{\text{CM}}(\Sigma) = a_1 \Sigma^k \left((1 + a_2 \Sigma)^m - 1 \right)^n, \quad \text{where} \quad (8)$$

$$\begin{aligned} a_1 &= 24.868, \quad a_2 = 0.097666, \\ k &= 0.14972, \quad m = 0.18931, \quad n = 1.8503. \end{aligned} \quad (9)$$

The comparison with the CGM model published later is simplified if one considers a change of variable from Σ to S . In that case

$$\Phi^{\text{CM}}(S) = b_1 S^k \left((1 + b_2 S)^m - 1 \right)^n, \quad \text{where} \quad (10)$$

$$\begin{aligned} b_1 &= 14.288, \quad b_2 = 0.0024115, \\ \text{and } k, m, n &\text{ are the same as above.} \end{aligned} \quad (11)$$

While the asymptotic behavior of both MLT and CM models are equal, i.e. they fulfill the limiting relations $k + mn \simeq 1/2$ and thus

$$\Phi(S) \sim S^{1/2} \quad \text{for} \quad S \gg 1 \quad (12)$$

as well as $k + n \simeq 2$ and hence

$$\Phi(S) \sim S^2 \quad \text{for} \quad S \ll 1, \quad (13)$$

a distinguishing feature of $\Phi^{\text{CM}}(S)$ is to yield about 10 times more flux than (7) for $S \gg 1$, i.e.

$$\Phi^{\text{CM}}(S) \sim 10\Phi^{\text{MLT}}(S) \quad \text{for} \quad S \gg 1 \quad (14)$$

while

$$\Phi^{\text{CM}}(S) \sim 0.1\Phi^{\text{MLT}}(S) \quad \text{for} \quad S \ll 1. \quad (15)$$

The function Φ^{CM} defined by (8)–(9) (or (10)–(11)) is only the first ingredient of the “CM model”. Because Φ is computed as a function of local variables (4), it depends on a characteristic length scale which cannot be provided by the formalism itself. Following the physical argument that the Boussinesq approximation leaves no natural unit of length other than the distance to a boundary and that eddies near the boundary of the convection zone are smaller than in the middle of the same (stacking), Canuto & Mazzitelli (1991) proposed to take

$$l = z \quad (16)$$

where z is the distance to the nearest stable layer. The combination of (8)–(9) and (16) has subsequently been called the “CM model”. In this form it was implemented by Kupka (1996) into ATLAS9 and used for the model grid computations presented here, although other prescriptions of l had been implemented and experimented with as well.

In a subsequent paper, Canuto et al. (1996) proposed a different FST convection model which avoided the usage of a growth rate. Rather, it was taken into account that the rate of energy input which feeds the velocity fluctuations and thus keeps convection from decaying is controlled by both the source of instability (buoyancy) and by the turbulence it generates. However, the treatment of the non-linear interactions had to be more simplified to keep the analytical model manageable. The equations of the turbulence model were solved in the limit for low Pr numbers. The new self-consistently computed input rate results in an increase of the convective flux for a given efficiency S which is largest at intermediate values of $S \sim 300$. For that reason a more complicated analytical fit formula had to be used to represent the predictions of the turbulence model to an accuracy better than 3% for all values of S . The CGM expression for Φ reads

$$\Phi^{\text{CGM}} = F_1(S)F_2(S) \quad (17)$$

where $F_1(S)$ has the same structural form as in the CM model,

$$F_1(S) = (\text{Ko}/1.5)^3 a S^k ((1 + bS)^m - 1)^n, \quad \text{with} \quad (18)$$

$$\begin{aligned} a &= 10.8654, b = 0.00489073, \\ k &= 0.149888, m = 0.189238, n = 1.85011, \end{aligned} \quad (19)$$

while $F_2(S)$ is given by

$$F_2(S) = 1 + \frac{cS^p}{1 + dS^q} + \frac{eS^r}{1 + fS^t}, \quad \text{with} \quad (20)$$

$$\begin{aligned} c &= 0.0108071, d = 0.00301208, \\ e &= 0.000334441, f = 0.000125, \\ p &= 0.72, q = 0.92, r = 1.2, t = 1.5. \end{aligned} \quad (21)$$

Here, Ko is the Kolmogorov constant which has been taken 1.7 in all our calculations, a value well inside of the experimental range (Praskovskiy & Oncley 1994). Note that Φ^{CGM} shows the same asymptotic behavior as Φ^{MLT} and Φ^{CM} in the limits of $S \ll 1$ and $S \gg 1$. Moreover, the CM and CGM functions Φ approach these limits in a very similar manner, because $F_2(S) \rightarrow 1$ for both very large and very small S , and the power exponents k, m, n of (9), (11), and (19) are almost identical. However, while

$$\Phi^{\text{CGM}}(S) \sim \Phi^{\text{CM}}(S) \quad \text{for } S \gg 1, \quad (22)$$

the low efficiency results differ, as

$$\Phi^{\text{CGM}}(S) \sim 0.3\Phi^{\text{MLT}}(S) \quad \text{for } S \ll 1 \quad (23)$$

(cf. (15)). On a logarithmic scale, the low efficiency limit of (17) is almost exactly the average of the fluxes of (7) and (10)–(11). The second difference between the two FST convection models is the choice of the scale length l which Canuto et al. (1996) have proposed to be

$$l = z + \alpha^* H_{p,\text{top}}. \quad (24)$$

This accounts for the observed fact that convection penetrates into neighboring stable regions and thus the scale length cannot decay to zero right at the layer where the stratification becomes stable according to the Schwarzschild criterion. The additional term in (24) is thus supposed to account for overshooting and provides a possibility for small adjustments, if exact stellar radii are needed, e.g. in helioseismology. However, the meaning of overshooting in this context must not be confused with the overshooting option offered by the ATLAS9 code. This point deserves special attention to which we turn in the following.

3.3. Length scale parameters and overshooting

The term $\alpha^* H_{p,\text{top}}$ in (24) accounts for the increase of the efficiency of convection due to convective penetration at the boundary between a stably and an unstably stratified region compared to a rigid boundary, for instance a fixed plate. The stellar scenario thus implies to increase the scale length l which can no longer be forced to zero as in (16). The total flux within convectively stable layers is still taken equal to the radiative flux. On the other hand, the overshooting prescription included in Kurucz (1993, 1998) as illustrated in Castelli et al. (1997) was invented to take into account that overshooting directly changes the temperature gradient also in a stable region next to a convection zone. The procedure suggested is to simply smooth out the convective flux over as much as $0.5 H_p$ in each direction around the last point where $\nabla = \nabla_{\text{rad}}$. This mimics the well-known property found in many numerical simulations (e.g. Hurlburt et al. 1986, 1994) and in solutions of the nonlocal Reynolds stress equations (Kupka 1999; Kupka & Montgomery 2002) where $F_{\text{conv}} > 0$ even though $\nabla - \nabla_{\text{ad}} < 0$ in layers right next to a neighboring convection zone. A steeply decaying F_{conv} cannot be modeled this way while the adjacent region where $F_{\text{conv}} < 0$ has to be neglected by taking $\nabla = \nabla_{\text{rad}}$. The effect of this flux smoothing procedure of ATLAS9 on the emergent flux is large enough to provide an additional degree of freedom to improve the match of solar observations by adjusting the smoothing width.

In the CGM model, the parameter α^* of (24) is typically of order 0.1 and may be slightly changed to compensate for uncertainties in opacities and in the treatment of convection. Values of 0.08 and 0.09, similar to Canuto et al. (1996), were used for the different grids presented in Sect. 4. However, the effect of such small changes is minute. No inconsistencies were found in a recent work by Montalbán et al. (2001) when model atmospheres computed with $\alpha^*=0.09$ were matched on top of stellar en-

velopes at different τ_{Ross} , despite a slightly larger value was used in the stellar structure computations to obtain the correct solar radius when using the most recent opacity data. On the other hand, using α^* to compensate for the Boussinesq approximation and various homogeneity assumptions in ATLAS9 by a match to, say, the entropy jump near the stellar surface as found from numerical simulations (cf. Ludwig et al. 1999 who used a combination of the CM fluxes (8)–(9) and the scale length (24)) may require larger variations for models very different from the sun. However, such a procedure cannot bring the temperature gradient of ATLAS9 model atmospheres into agreement with the simulations. The latter avoid horizontal homogeneity assumptions but cannot be afforded together with a treatment of frequency dependent radiative transfer which is comparably sophisticated as that one used in ATLAS9. Hence, emergent fluxes, spectra, and photometric colors will be different as well. As long as such a matching procedure is not shown to allow an improved match of fundamental star data over extended parts of the HR diagram (and thus improving over present models, cf. various publications discussed in Sect. 2), its practical advantages appear more limited. For that reason, we have preferred to use the CGM model as intended by its authors and studied grids with a constant α^* which makes them suitable to be matched with stellar structure calculations using the same treatment of convection (Montalbán et al. 2001).

3.4. Implementation of FST models into ATLAS9

In the ATLAS9 implementation of the CGM convection model the quantities (17)–(21) are actually computed as functions of Σ . Thus, only minimal changes were necessary in the subroutine TCORR, which performs the temperature correction, and in CONVEC, which computes the convective flux, for replacing the CM with the CGM model. TCORR and CONVEC were also the only subroutines that had to be changed for implementing the CM model into ATLAS9. The scale length of the CGM model is evaluated in the following way:

$$l = \min(z_{\text{top}} + \alpha^* H_{p,\text{top}}, z_{\text{bottom}} + \alpha^* H_{p,\text{bottom}}) \quad (25)$$

This choice makes convection slightly more efficient in comparison with (24) and more consistent with the idea of accounting for overshooting, as the latter is also expected to occur below convection zones. For most model atmospheres we found that the differences between these alternative prescriptions are either zero or negligibly small, because the temperature gradient for convection zones which are entirely contained within the atmosphere is practically radiative while for convection zones extending below the atmosphere the evaluation of l in a pure model atmosphere code necessarily has to occur at the top of the convection zone.

We note here that in principle (8)–(9) and (17)–(21) could also be used together with the common scale length $l = \alpha H_p$ with $\alpha < 1$, or other scale lengths. Results on such calculations will be reported in Kupka et al. (2002).

3.5. Turbulent pressure and the optically thin limit

For the CM model, a prescription for the turbulent pressure was published as well, although the results were given only for $S \gg 1$ and in tabular form. In stellar atmospheres, $S \gg 1$ is usually attained only in cool stars and close to the bottom where the Rosseland mean optical depth $\tau_{\text{Ross}} > 10$. Hence, the ATLAS9 implementation of the CM model does not account for turbulent pressure. On the other hand, for the CGM convection model analytical fit formulae for v_{turb} and p_{turb} were published by Canuto et al. (1996) which can be used even for $S \ll 1$ and were implemented into ATLAS9 as well. A number of model atmospheres for A to early M type dwarfs and for giants were computed with the CGM model with and without the prescription of p_{turb} . Differences were found only for stars with deep envelope convection zones, although in most cases both T and P changed by less than 0.1% for $\tau_{\text{Ross}} < 5$, and by no more than 0.5% to 1% for $10 < \tau_{\text{Ross}} < 100$. As the inclusion of p_{turb} slowed down the convergence of models while spectra and colors remained indistinguishable from the case $p_{\text{turb}} = 0$, all the CM and CGM model atmospheres grids presented here are computed without a p_{turb} , just as their MLT counterparts. We note that for stellar structure calculations the change in temperature structure due to p_{turb} may be more important than for flux predictions derived from ATLAS9 model atmospheres. To avoid discrepancies with the CGM treatment as used in the model grids a reasonable compromise is to match model atmospheres and stellar envelopes at a $\tau_{\text{Ross}} \sim 10$.

Following a suggestion by Canuto (private communication) the correction of Spiegel (1957) for radiative losses in optically thin media was implemented for the case of the CM model. However, except for late K and early M dwarfs, where ATLAS9 models are not reliable any more due to the dominance of molecular lines, the effects were found to be negligible. The primary reason for this are the very low values of F_{conv} predicted by the CM model for $\tau_{\text{Ross}} < 2$ for stars with $T_{\text{eff}} > 4000$ K. For the CGM model, convection is slightly more efficient, but still the effects of such a correction are expected to be very small. Therefore, no further experiments with radiative loss rates were made with FST convection models. The case is different for MLT where the results are more sensitive to the different cooling rates of “optically thin bubbles”, as

$$\Phi^{\text{MLT}}(S) > \Phi^{\text{CGM}}(S) > \Phi^{\text{CM}}(S) \quad \text{for } S \lesssim 10 \quad (26)$$

because of (15) and (23) and due to the much larger l of MLT for $\alpha > 1$ if $z < H_p$. A correction of F_{conv} for the optically thin limit is always included in the MLT implementation of ATLAS9 (Kurucz 1993; Castelli et al. 1997).

4. Model grid computation

Two model grids have been computed independently at the Paris and Vienna observatories.

At the Paris Observatory an automatic procedure was created by one of the authors (DK). The procedure is interactive, and allows the computation of grids of model atmospheres based on the ATLAS9 code, of Balmer line profiles, surface fluxes and intensities, colors and synthetic spectra, all in one run. The flux and temperature computations are iterated until the following convergence criteria are satisfied: the maximum of the flux and flux derivative errors have to be equal to or less than one and ten percent, respectively. In addition, the maximum of the temperature correction has to be equal to or less than one K.

In the MLT case, we started from the original Kurucz grids (Kurucz 1993, 1998) and recomputed the models by the scaling procedure of the ATLAS9 code. The thickness of the layers of the model atmospheres was divided by 2 or 4 in comparison with the original Kurucz (1993, 1998) models, in order to solve numerical instabilities in the iteration procedure for the flux computation, and to provide more accurate photometric colors (see Sect. 5.2.2 and next paper in this series). Models with higher resolution converged faster and smaller flux errors were achieved.

The parameters used for these model grids are given in Table 1. We recall that the metallicity is given in terms of the logarithmic ratio between the total number of atoms of each species, except for hydrogen and helium, over the number of hydrogen atoms, with respect to the solar metallicity defined in the same way. For instance, $[M/H]=0.0$ and -1.0 means that the opacities entering the model calculations are computed using either solar element abundances or solar element abundances divided by 10 for all elements other than hydrogen and helium. The MLT models were computed for two values of α , the original value used by Kurucz $\alpha = 1.25$, and the lower value $\alpha = 0.5$, chosen for reasons given in Sects. 3 and 5.

In the CM and CGM cases, we started from our MLT models with $\alpha = 0.5$, and computed grids with the same set of parameters. For the CGM convection a value of $\alpha^* = 0.08$ was chosen (see Sect. 3 for a discussion).

At the Vienna Observatory, model grids with several combinations of convection treatment and vertical resolution were computed for slightly smaller step sizes in T_{eff} , larger step sizes in $\log g$ and more $[M/H]$ values. For MLT models a value of 0.5 has been chosen for α . Convection has been turned off for models with $T_{\text{eff}} \geq 8600$ K, because the convective flux can be neglected for higher temperatures, as can be seen from Fig. 4. As in the Paris grid the uppermost layer is located at $\log \tau_{\text{Ross}} = -6.875$. The difference of consecutive layers in $\log \tau_{\text{Ross}}$ is 0.125 and 0.03125 for models with 72 and 288 layers, respectively. In addition to the model atmospheres, fluxes and colors in 12 systems have been computed. Furthermore, information on the convergence extracted from the ATLAS9 output is provided for each model. The atmospheric and computational parameters are summarized in Table 1.

The grid computations were performed with the perl package SMGT (Stellar Model Grid Tool), described

in Schmidt (1999)¹. This non-interactive program runs ATLAS9 repeatedly until the convergence criteria are satisfied for each model. The output of ATLAS9 is evaluated directly and selected information is provided for each model, such as the root mean square (RMS) and maximum values of the flux and flux derivative errors, the maximum of the convective to total flux ratio, the extension of the convection zone, and the optical depth where the temperature equals T_{eff} . The grids defined in Table 1 are available on CDROM on request from the authors.

We note here that two different, but overlapping grids of model atmospheres were computed as there were different applications in mind. The main motivation for the computation of the Paris grids was to calculate photometric colors and their derivatives with respect to T_{eff} and $\log g$, which will be used in view of seismic applications (Watson 1988; Garrido et al. 1990; Balona & Evers 1999). This required rather small steps in $\log g$, but a restricted range for T_{eff} and few metallicity values. The results of this specific application will be discussed in a subsequent paper of this series. The Vienna grids, on the other hand, are intended for general use, which is the reason for choosing intermediate values for the parameter step sizes and covering as much of the HR diagram as possible. Examples for already published applications of these grids can be found in Montalbán et al. (2001, see below) and in D’Antona et al. (2002).

4.1. Resolution

To show that for specific applications it is necessary to use the models with 288 layers, we examined the quantity $\Delta z = z(\tau_{\text{Ross}} = 3.162) - z(F_{\text{conv}} = 0)$, where z is the depth (distance from top layer) in the atmosphere in km and $z(F_{\text{conv}} = 0)$ is the depth of the upper limit of the convection zone. This quantity has been used by Montalbán et al. (2001) for the calculation of the convective scale length in stellar interior models which use convective atmospheres computed with ATLAS9 as a boundary condition. It turned out that for a particular region in the HR diagram, calculating this quantity from atmospheric models with 72 layers results in unphysical oscillations in solar evolutionary tracks which disappear for higher resolutions (J. Montalbán, private communication). Fig. 1 shows the values of Δz for a small grid of CGM model atmospheres with $[M/H]=0$, $T_{\text{eff}}=4200 \dots 4800$ and $\log g=3.0 \dots 3.6$ for four different resolutions, with the stepsize $\Delta \log \tau_{\text{Ross}}$ divided by two for each successive resolution value. For 144 layers, the results are rather different from the 72 layer ones (note the peak at $(T_{\text{eff}}, \log g) = (4400, 3.2)$). There is a small change when increasing to 288 layers, whereas the change when using 576 layers is negligible. This shows that 288 layers are sufficient in low to moderate temperature atmospheric models, in particular as all structural

¹ A summary is given in the Appendix and directions for the use of this program can be found at http://ams.astro.univie.ac.at/~heiter/smgt_usage_1.html.

Table 1. Atmospheric and computational parameters of the model atmosphere grids.

Paris				Vienna			
	Min	Max	Step	Min	Max	Step	
T_{eff} [K]	6000	8500	250	4000	10000	200	
$\log g$	2.0	4.5	0.1	2.0	5.0	0.2	
[M/H]	-1.0, 0.0, +1.0			-2.0, -1.5, -1.0, -0.5, -0.3, -0.2, -0.1, 0.0, +0.1, +0.2, +0.3, +0.5, +1.0			
v_{micro} [km s ⁻¹]	2			0 ^b , 1 ^b , 2, 4			
Convection	MLT	CGM	CM	MLT	CGM	CGM	CM
Parameter	1.25, 0.5	0.08		0.5	0.09		
$\Delta \log \tau_{\text{Ross}}^a$	0.0625 or 0.03125			0.125	0.125	0.03125	0.03125
Number of layers	143 or 285			72	72	288	288

^a $\log \tau_{\text{Ross}}(\text{top}) = -6.875$

^b in preparation

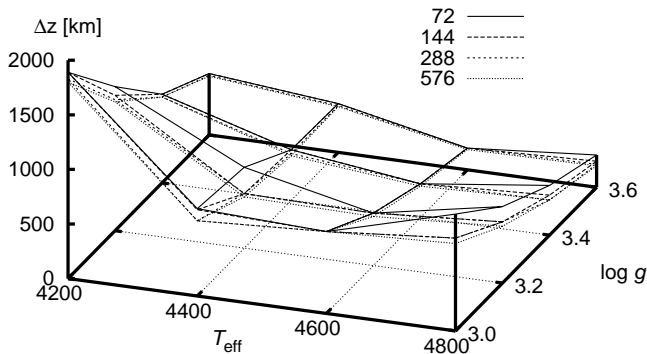


Fig. 1. $\Delta z = z(\tau_{\text{Ross}} = 3.162) - z(F_{\text{conv}} = 0)$ for a CGM model grid with four different numbers of layers equally distributed between $\log \tau_{\text{Ross}} = -6.875$ and $+2$. This quantity is used for the calculation of the convective scale length in stellar interior models and the graph shows its sensitivity to depth resolution in this part of the HR diagram.

quantities (e.g. the temperature gradient ∇) are resolved. For models with $T_{\text{eff}} \geq 10000$ K, on the other hand, we verified that 72 layers are sufficient.

5. The effects of Convection Treatment

5.1. Effects on model atmosphere structure

We first examine changes of temperature and convective flux distribution when using different convection models. Figs. 2, 3, and 4 show the intricate dependence of the effect of convection treatment on T_{eff} , $\log g$, and [M/H] of the model.

Fig. 2 displays the temperature and the convective flux as a function of Rosseland optical depth ($\log \tau_{\text{Ross}}$) corresponding to the models used for three specific main sequence solar metallicity stars which have been chosen so as to cover the temperature range of interest: the Sun, Procyon – a well studied reference star, and β Ari – a well observed hot star. For each star, several models are computed which differ only for the convection treatment. T_{eff} , $\log g$, metallicity, and microturbulent velocity of the models are taken from previous detailed analyses (by CV

for β Ari, van 't Veer-Menneret et al. (1998) for Procyon and Kurucz (1998) for the Sun).

The slope of the $T - \tau$ relation within the CZ indicates the efficiency of the convection transport. It is steeper for a less efficient convection, i.e. a temperature gradient closer to the radiative one. For instance, in Fig. 2a, it can be seen that the CM model predicts the least efficient convection, followed with increasing convective efficiency by the MLT ($\alpha = 0.5$), the CGM and the MLT ($\alpha = 1.25$) models. The same trend is observed for the convective flux in Fig. 2b. This is a consequence of the fact that radiative losses of the convective fluid are always large within the stellar atmosphere where the gas is optically transparent. Hence, the inequality chain (26) always holds at least at lower optical depths ($\tau \lesssim 1$). The scale lengths (1), (24), (16) of MLT, CGM and CM respectively also obey such an inequality chain for distances z closer to stably stratified layers than αH_p and for the ranges of α and α^* considered in our work. Therefore, the amount of convective flux and the associated $T - \tau$ relations shown in Fig. 2 are an immediate consequence of these inequality chains.

For hotter stars ($T_{\text{eff}} \simeq 8000$ K), as the convective efficiency decreases, all convection models predict a temperature gradient close to the radiative one.

The effect of convection treatment on the atmosphere structure depends on metallicity, gravity and T_{eff} in a complex way, as illustrated in Fig. 3. Evidently, a metal rich atmosphere reduces the efficiency of the convection transport, as does a low gravity, or a high T_{eff} . The influence of $\log g$ on the convective efficiency depends strongly on T_{eff} , [M/H], and the convection model. For instance, a model at $T_{\text{eff}} = 6500$ K, $\log g = 2.5$, $\alpha_{\text{MLT}} = 0.5$, and ten times solar metallicity is completely radiative (see Fig. 3a, thin dashed lower line), while for $\log g = 4.5$ and identical parameters otherwise a small deviation from radiative stratification is found (thick dashed lower line). This deviation grows significantly when decreasing the metallicity to one tenth of the solar one (Fig. 3b).

The variation of the maxima of the convective flux with T_{eff} , $\log g$, and [M/H] is shown in Fig. 4 for the CGM models. The decrease of convective flux with increasing metallicity is a consequence of the lower mass density (ρ)

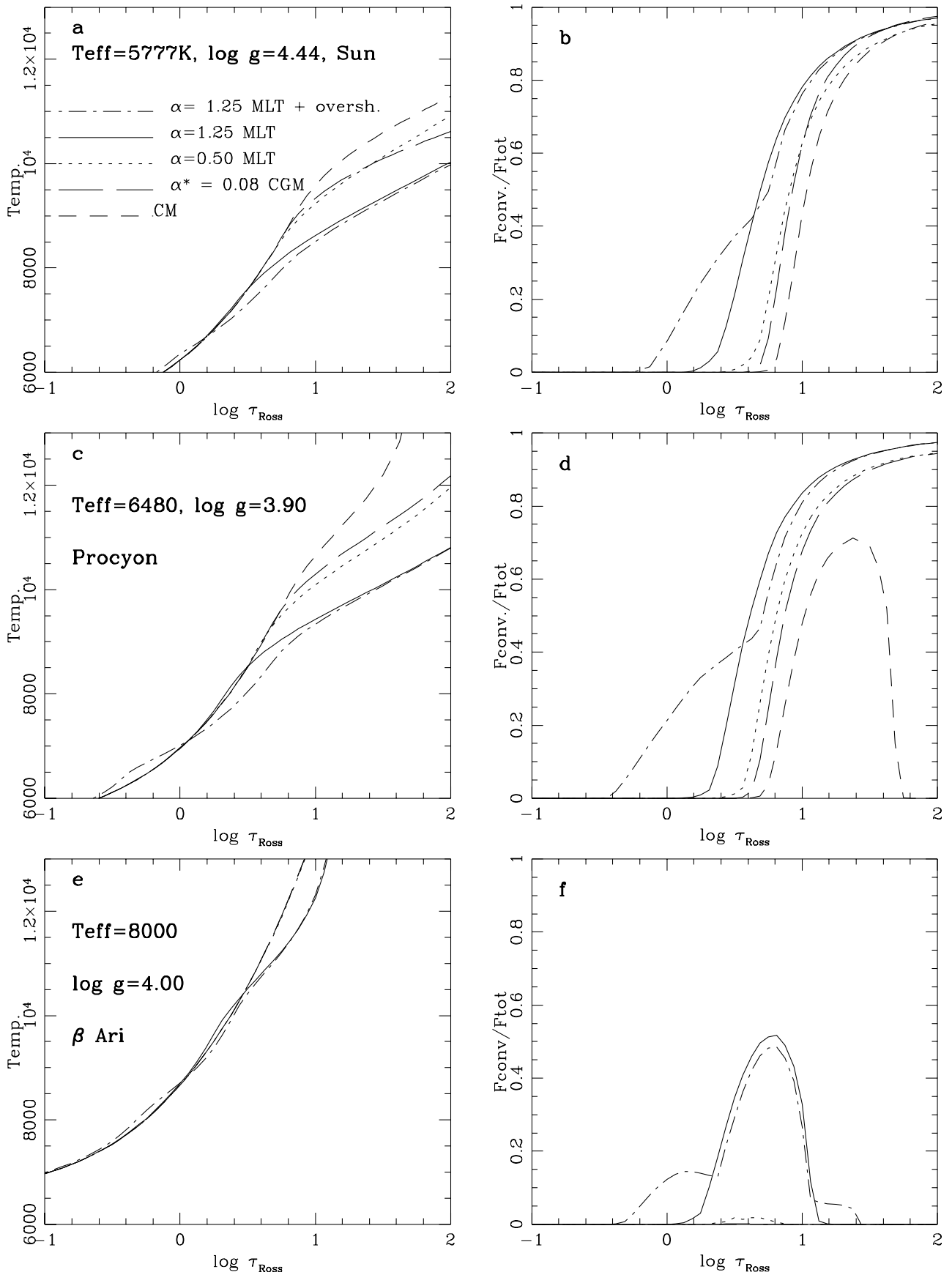


Fig. 2. Distributions of temperature (left panels) and ratio of convective to total flux (right panels) with Rosseland optical depth for the three model atmospheres adopted for the Sun (a, b), Procyon (c, d) and the A5V star β Ari (e, f). For each star we show five models computed using different convection treatments.

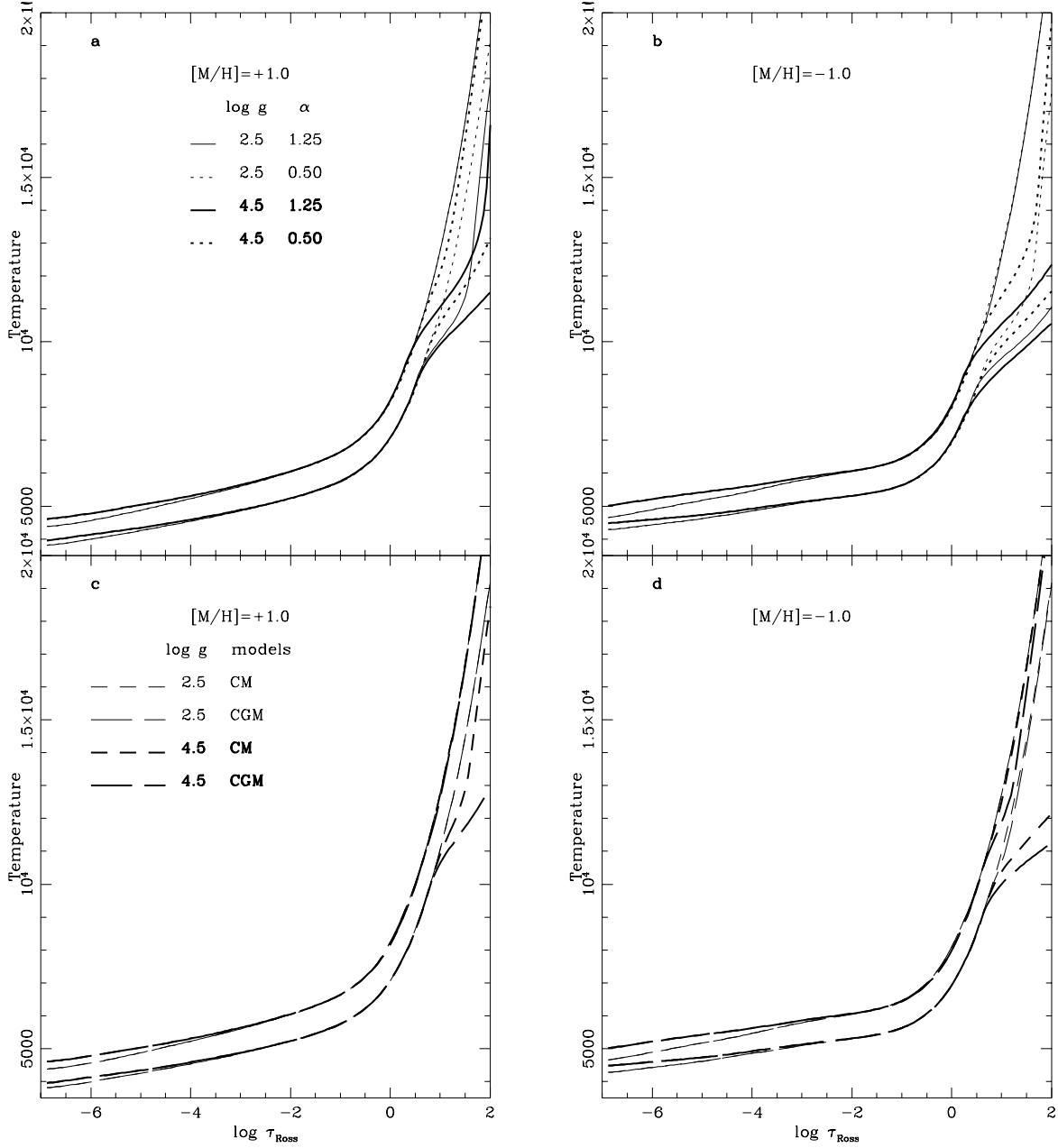


Fig. 3. Temperature versus Rosseland optical depth for models with two different $\log g$ values, computed with MLT without overshooting (a: $[M/H] = +1$, b: $[M/H] = -1$, two different values of α for each $[M/H]$) and with FST convection formulation (c: $[M/H] = +1$, d: $[M/H] = -1$, CM and CGM for each $[M/H]$). The models are represented for two different values of T_{eff} in each panel, using the same line styles: 7500 K for the upper four curves and 6500 K for the lower four curves.

found in metal rich atmospheres. The latter is a result of the increased opacity, which requires a smaller column density for a given optical depth. Due to increased line blanketing in metal rich atmospheres, the requirements of flux constancy and hydrostatic equilibrium then result in both lower temperature and lower pressure in the outermost layers. As a consequence, lower densities are also found near the boundary of the CZ. This makes convection less efficient, although this effect is partially compen-

sated by a higher convective velocity found for metal rich atmospheres. Fig. 4 also shows the influence of using a four times higher resolution in optical depth, resulting in a much smoother run of the curves and in a small shift towards lower temperatures.

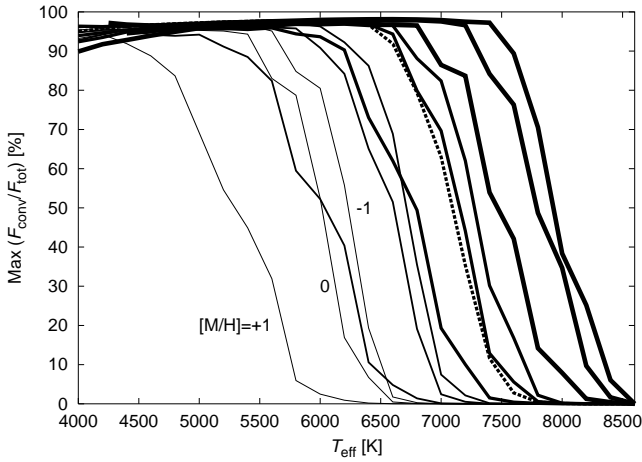


Fig. 4. Maximum of convective to total flux ratios as a function of T_{eff} , for the following values of $\log g$: 2, 3, 4, 5, represented by increasing line thickness, and three different metallicities as labeled for $\log g=2$, with the same trends for the other values. The dashed curve was computed with $[M/H]=0$ and $\log g=4$, but with a four times higher depth resolution. The CGM convection model was used in all cases.

5.2. Consequences on observable quantities

5.2.1. Balmer line profiles

The effect of changing the physical parameters entering the models on the Balmer line profiles (BLPs) is very complex. This is illustrated in Fig. 5, where the synthetic profiles for several different convection models are compared to the observed ones for the same three stars as in Fig. 2. The spectra shown in Fig. 5 were obtained at the Haute-Provence Observatory, with the spectrograph Aurèlie attached to the 152cm reflector, equipped with a CCD receptor. The resolution is about 25000. The Aurèlie spectra are observed in the first or second order, depending on the wavelength. The wavelength range is 200 Å, and the continuum tracing is local, using the most suitable windows. With a signal to noise ratio of at least 400 we can expect an accuracy for the continuum location of 0.3 %, i.e. 0.5 % for the ratio of line to continuum fluxes in the line wings. This corresponds to a 30 to 60 K change in effective temperature for F to G stars.

In the case of H_{α} the effects are never larger than 0.5%. Fig. 5 shows that the H_{α} profile is insensitive to the choice of any of the scale lengths or convection models discussed in Sect. 3, while in the case of H_{β} the profiles computed with MLT and $\alpha = 1.25$ are too narrow. As an example, in the case of Procyon this H_{β} profile must be computed with T_{eff} around 300 K higher to represent the observed profile. The insensitivity of H_{α} to any convection treatment is one of the reasons why it is a very good temperature indicator. However, it is formed close to the boundary of convectively unstable layers and therefore can be modified by inclusion of overshooting.

Fig. 5 is a convincing illustration that by the use of the CM or CGM convection treatment, the observed H_{α} and

H_{β} profiles can be represented by the same atmosphere model, and this constraint can be achieved in the MLT case provided a value for α of about 0.5 is adopted. Thus, we want to emphasize that for the three stars investigated here, *less efficient convection within ATLAS9 type model atmospheres allows the best fit of H_{α} and H_{β} using the same atmosphere model.*

In the MLT case, the consequences of these effects on the BLPs have been extensively described by VM and Fuhrmann et al. (1993), who demonstrated that the BLPs are sensitive probes of the atmosphere structure and of effective temperature for late A, F, and G dwarf stars. Fig. 6a,b illustrates the effect of changing the MLT parameter α on the BLPs, and to what extent this modification depends on the model parameters. This sensitivity strongly depends on the selected combinations of the model parameters. For instance, the largest differences are seen for models with T_{eff} between 7000K and 8000K, $\log g = 4.5$ and high metallicity. In contrast, the differences are insignificant at low gravity, high metallicity and high temperature. The shape of the profiles is also affected, the most for low temperature and low metallicity models.

Fig. 6c,d shows the difference between two H_{β} line profiles, computed with MLT and CM. The difference between the CGM and CM H_{β} profiles was not plotted, because it is similar to MLT($\alpha = 0.5$) – CM. The differences with MLT($\alpha = 1.25$) are the largest and strongly depend on temperature and gravity, but less on metallicity. These statements mean that the most efficient convection treatment is MLT with $\alpha = 1.25$, in agreement with the $T - \tau$ laws shown in Figs. 2 and 3. From the observer’s point of view, Fig. 6a-d also reveals that Balmer line profiles have to be measured and normalized to an accuracy of at least 0.5% to draw a clear distinction between convection models with different efficiency. Insufficiently determined profiles may thus easily introduce erroneous trends or large scatter when analyzing their dependence on a particular convection treatment.

We stress here that the sensitivity to MLT’s parameter α strongly depends on gravity. For instance, for $T_{\text{eff}} \leq 7500$ K all convection models with low gravity yield inefficient convection. This is due to the fact that low gravity implies lower densities, and the convective efficiency is related to the density as explained in subsection 5.1 above. Moreover, we suggest to consider the *commonly assumed insensitivity of BLPs to gravity change for T_{eff} below 8000 K with real caution.* Indeed, Fig. 7 shows clearly that the sensitivity of BLPs to gravity changes depends more than usually expected on metallicity, T_{eff} , and finally on all parameters playing a role in the efficiency of the convective transport. It depends also on the gravity itself, the second derivative is not zero. This effect is most important for the highest metallicity and largest T_{eff} . The main reason is that an increase of metallicity leads to a lowering of the density on the one hand while a higher effective temperature favors radiative transfer on the other.

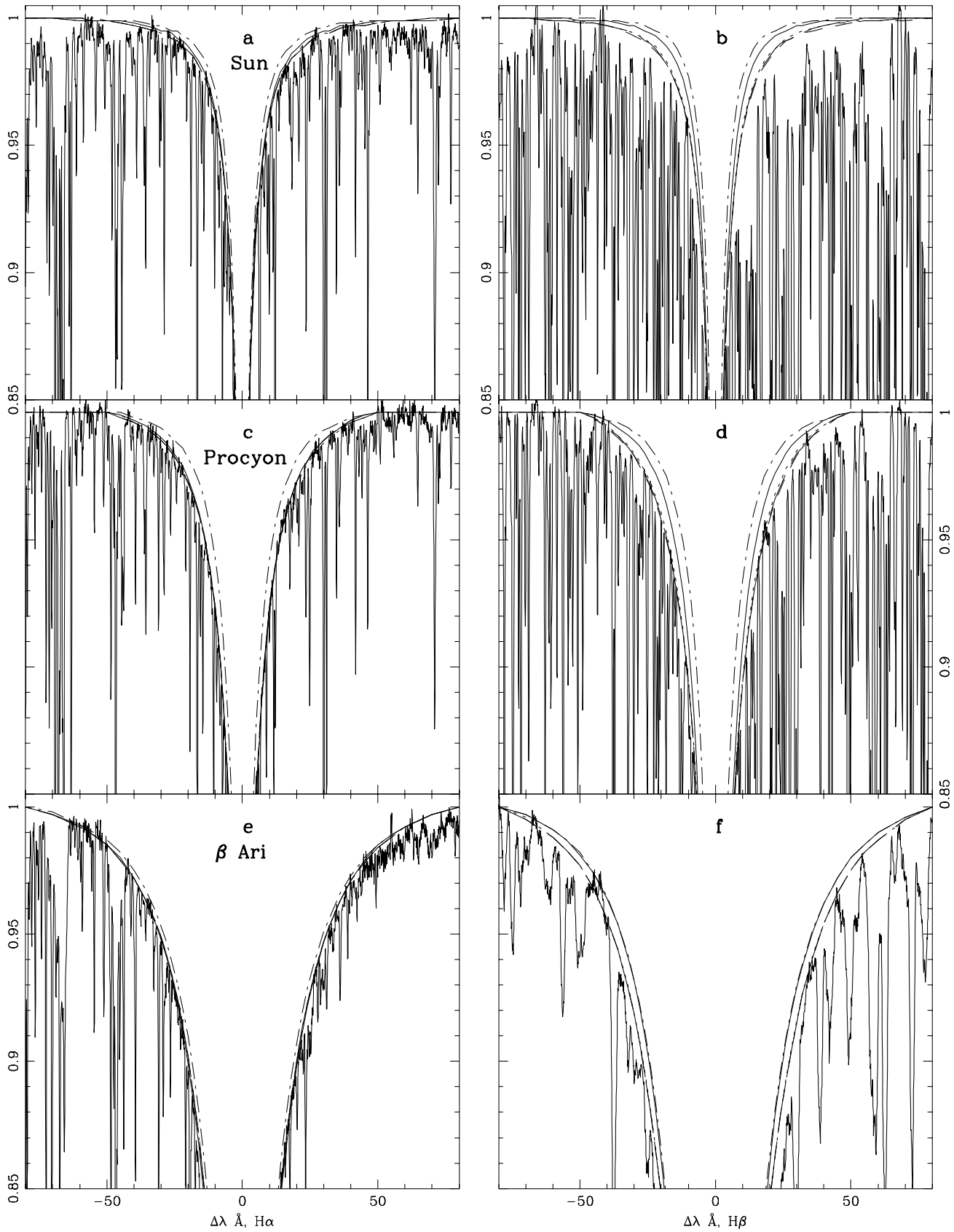


Fig. 5. H_α (left panels) and H_β (right panels) line profiles computed with different convection models represented by the same line styles as in Fig. 2, together with the observed profiles for the same three stars as in Fig. 2.

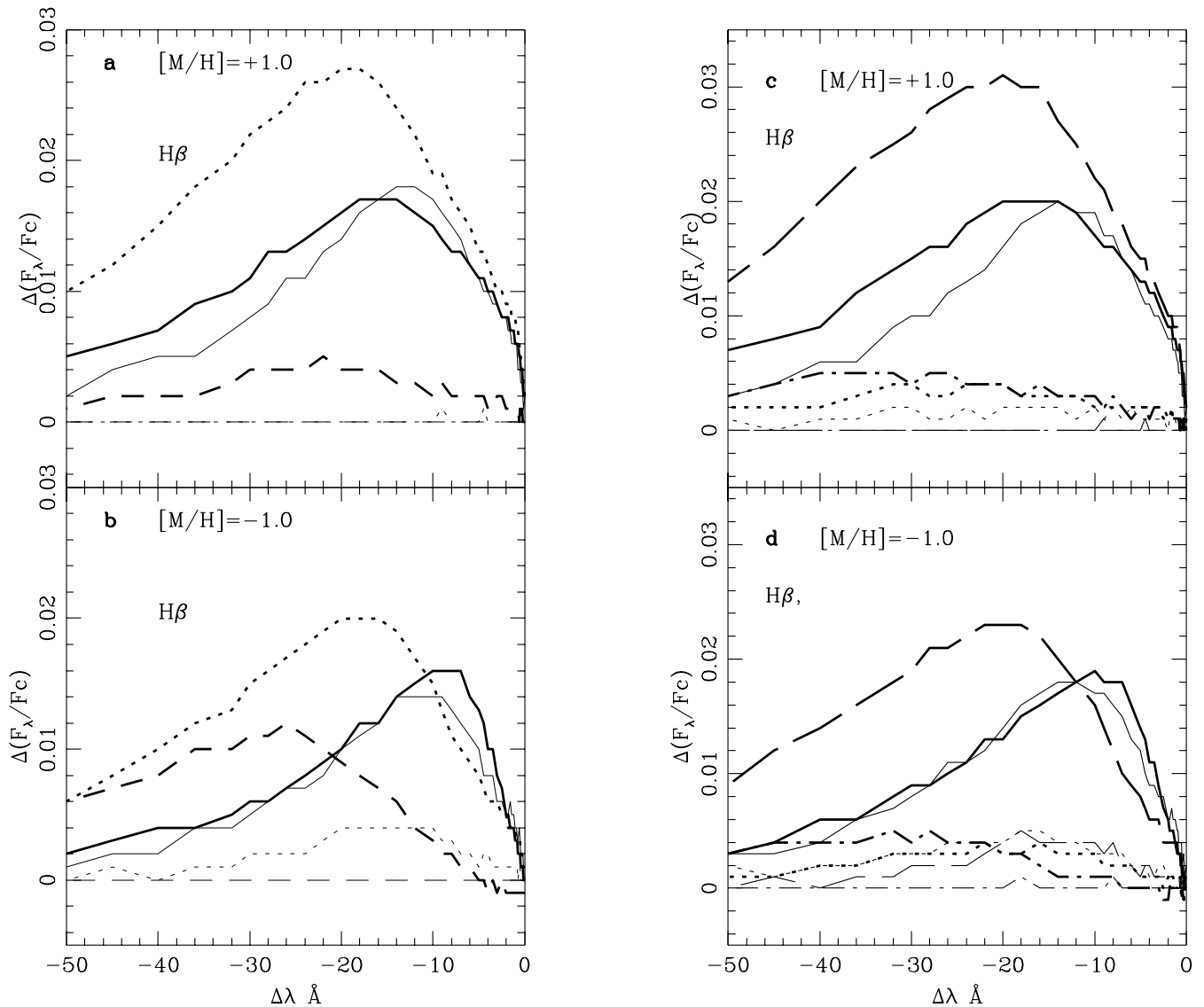


Fig. 6. Differences between normalized fluxes in Balmer line profiles obtained from two models differing only by the convection treatment, versus the distance from the line center $\Delta\lambda$ in Ångstrom units. Fluxes are normalized to the local continuum flux F_c . The two left panels display the difference of fluxes computed using MLT models differing by the α parameter: $F(\alpha = 1.25) - F(\alpha = 0.5)$ for two metallicities. The different line styles correspond to different T_{eff} 's: full lines for 6500 K, dotted lines 7500 K and short-dashed ones 8500 K, and thin and thick lines respectively correspond to $\log g = 2.5$ and 4.5. In the right panels the models differ by the convection formulation, and are identifiable as follows: for MLT($\alpha = 1.25$)–CM full lines correspond to $T_{\text{eff}} = 6500$ K, long dashed lines to $T_{\text{eff}} = 7500$ K; for MLT($\alpha = 0.50$)–CM dotted lines correspond to $T_{\text{eff}} = 6500$ K, and short-dash-dotted lines to $T_{\text{eff}} = 7500$ K. Thin and thick lines have the same meaning.

5.2.2. Fluxes and colors

We have computed fluxes for solar models with different convection treatments as follows: CGM, CM, MLT ($\alpha=0.5$), MLT ($\alpha=1.25$), MLT ($\alpha=1.25$ with overshooting). The same parameters have been chosen for all models: $T_{\text{eff}} = 5777$ K, $\log g = 4.4377$, $v_{\text{micro}} = 1.5 \text{ km s}^{-1}$, element abundances from Anders & Grevesse (1989), except for Fe, for which the current value of $\log(N_{\text{Fe}}/N_{\text{tot}}) = -4.51$ was used (Kurucz 1998). To compare the calculated solar fluxes to observations, solar irradiance data have been taken from Neckel & Labs (1984), and in addi-

tion from two more recent sources: Lockwood et al. (1992, Lowell Observatory, 1985) and Thuillier et al. (1998, SOLSPEC spectrometer on ATLAS I mission, 1992). The irradiances in the region of maximum emitted radiation, i.e. 410 to 510 nm, are displayed in Fig. 8.

As can be seen, the three observational data sets are different from each other by up to 15 % (upper panel), although Neckel & Labs (1984) estimate 0.5 % as an upper limit for the local systematic error of their measurements. But they point out that intrinsic intensity variations depending on solar activity can occur when comparing measurements made at different times. These amount to 2 %

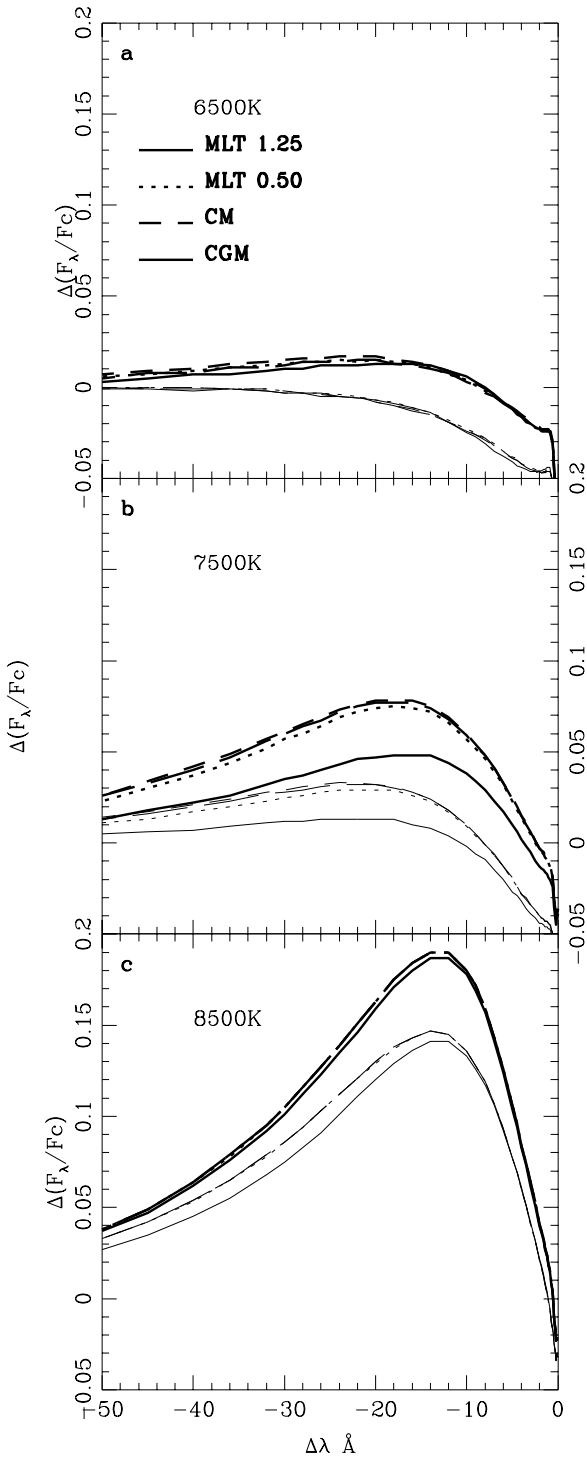


Fig. 7. Differences between H_{β} line profiles computed with $\log g = 2.5$ and 4.5 . Different convection models are represented by different line styles, for metallicities of -1 and $+1$ by thin and thick lines respectively, and for three effective temperatures.

in certain spectral regions (e.g. the CaII K line) in their data, which are derived from observations made over a 20 yr period (see also Livingston et al. 1991). For comparison, Lockwood et al. (1992) give an upper limit for the errors of their measurements of 2 % (their observations

were made at a phase of low solar activity), and Thuillier et al. (1998) quote a mean uncertainty of 2-3 % (data obtained at high solar activity)². Detailed discussions of the error sources and comparisons with previous observations are given in each of the three references.

However, the mean of the maximum relative difference between the irradiances from the three sources is 5 % in the region of 450 to 480 nm, which is much larger than the differences between the fluxes calculated with different convection models (2 %, cf. lower panel of Fig. 8). The CM and MLT ($\alpha=0.5$) fluxes are almost identical to the CGM flux. Therefore, the solar irradiance measurements cannot be used to decide between the various models. A similar conclusion would result if measurements of solar central intensity would be used, because the error estimates by Neckel & Labs (1984) for these measurements (the other two sources did not include this kind of measurements) are equal to that for the irradiance spectra. Thus, we regard tests of central intensity calculations against observations (e.g. Castelli et al. 1997) as having limited significance until accuracy and absolute calibration of these data will have been established with the necessary reliability.

The general dependence of the calculated flux on the convection model can be seen in Fig. 9, where the ratios of MLT and CGM to CM fluxes are displayed for two different values of T_{eff} and $\log g$ and the extreme case of $[\text{M}/\text{H}] = -1$. For all cases, the CGM flux is closest to the CM flux, followed by MLT ($\alpha=0.5$) and with a larger discrepancy by MLT ($\alpha=1.25$). The differences between the models are very small for the highest T_{eff} and lowest $\log g$ values. Otherwise they depend strongly on the wavelength range, and no general trend is visible. This is illustrated by Table 2, which lists the $(T_{\text{eff}}, \log g)$ combinations for three metallicities in order of increasing flux differences from top to bottom. Three different wavelength ranges have been regarded: blue, UV and red. It can be seen that in the latter two, the convective efficiency effect is inverted compared to the one in the blue part. Thus, one can only guess that the calculated emitted flux depends in a complex way on the combination of T_{eff} , $\log g$, and the convection model.

We use our grids of computed fluxes to derive colors and color indices in the *uvby* photometric system. The role of convection on this photometric system has already been studied by SK (see Sect. 2), also using the ATLAS9 code in the MLT and CM cases. Here, we extend this study to the CGM case, and investigate how the variations of color indices due to temperature and gravity variations are affected by the convection formulation.

We find that:

- there are no measurable differences between colors or indices computed with CM and CGM models and both are very close to those computed with MLT($\alpha=0.50$) models.

² Information on the solar activity level has been obtained from the National Solar Observatory Digital Library (<http://www.nso.noao.edu/diglib/ftp.html>).

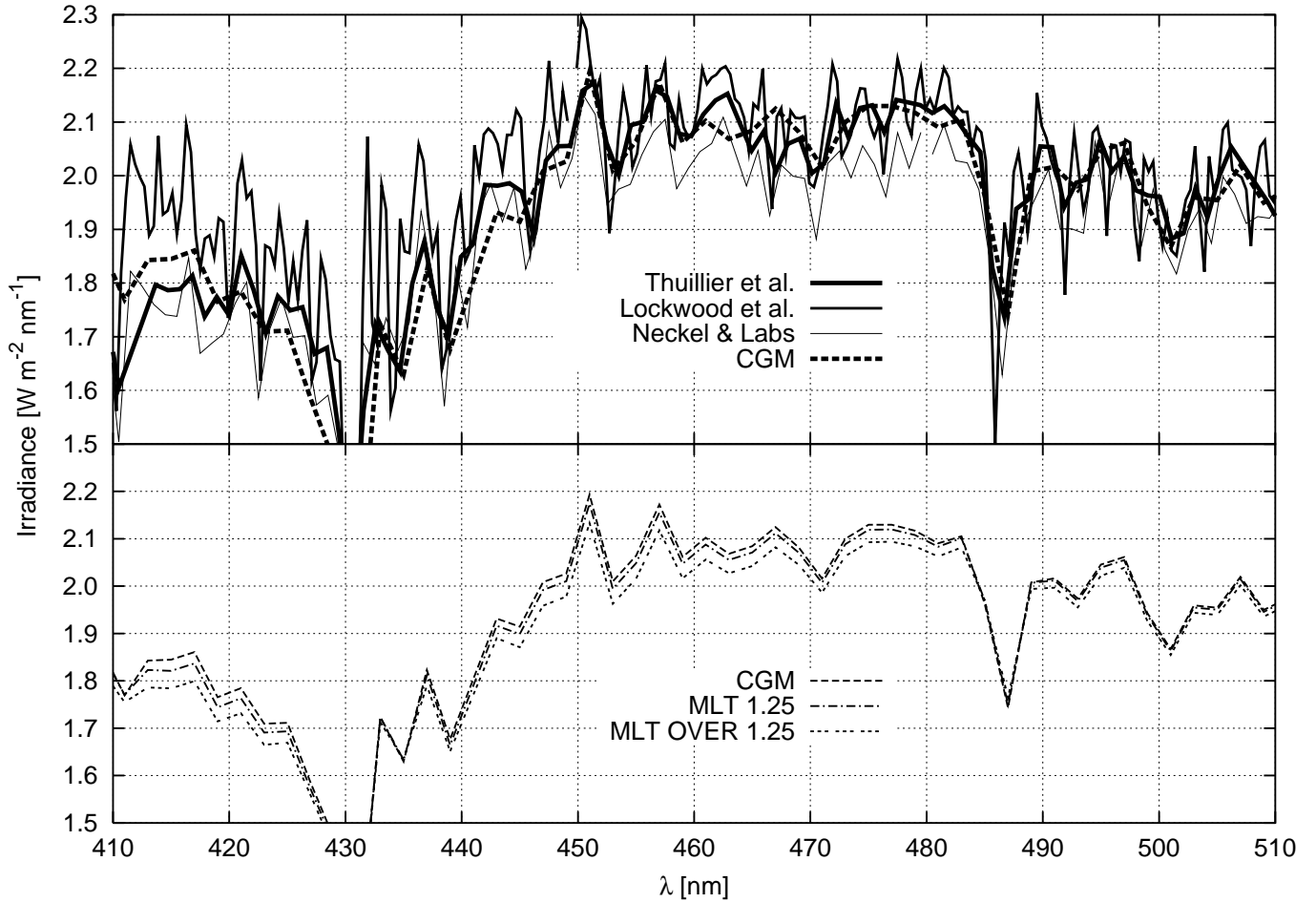


Fig. 8. *Top:* Observations of the solar irradiance from Thuillier et al. (1998), Lockwood et al. (1992) and Neckel & Labs (1984) (solid lines) and solar irradiance calculated with the CGM model (dashed line). *Bottom:* Solar irradiance calculated with three different convection models.

– differences become much more important if colors or indices computed with $MLT(\alpha=1.25)$ models are compared to those computed with CM, CGM, or $MLT(\alpha=0.50)$ models.

Thus, we can extend the results of SK (see Sect. 2) to the CGM model, and conclude that color indices computed with CGM models are generally in better agreement with observations than those computed with $MLT(\alpha=1.25)$ models.

The $(b - y)$ index is the most sensitive one with respect to temperature changes, and this sensitivity is also strongly influenced by the convection model considered. We have investigated the variation of $(b - y)$ indices computed using models differing only by the convection treatment. Fig. 10 shows that the sensitivity of $(b - y)$ to convection change is T_{eff} and gravity dependent, and the temperature changes associated with the ones of $(b - y)$ are written along the curves. The results are very similar, and in the same order of magnitude, for metallicities ten times or one tenth of the solar one. The same conclusion is reached when the CM model is replaced by the CGM or by $MLT(\alpha=0.50)$ formulation.

From this result we can establish that the “error” (or “change”) on temperature variation estimations can be important, i.e. as large as 200 K, when using $MLT(\alpha=1.25)$ instead of CM convection treatment (or CGM or $MLT(\alpha=0.50)$). It can reach up to 400 K, if the overshooting option of ATLAS9 is not removed.

6. Conclusions

One of the main conclusions to be raised from this study is that as long as one considers inefficient convection, whatever is the choice of the formulation, either MLT with low α , or FST, the interpretation of spectroscopic or photometric observations is equivalent: observed BLPs and Strömgren color indices of dwarf and subgiant stars between A5 and G5 spectral types, and in a large range of metallicity are best represented by the use of less efficient convection transport, i.e. MLT with $\alpha = 0.5$, or with FST formulation. This confirms results already obtained by Fuhrmann et al. (1993), VM and van ’t Veer-Menneret et al. (1998) for the Sun, Procyon, and other cool metal-poor stars using MLT models.

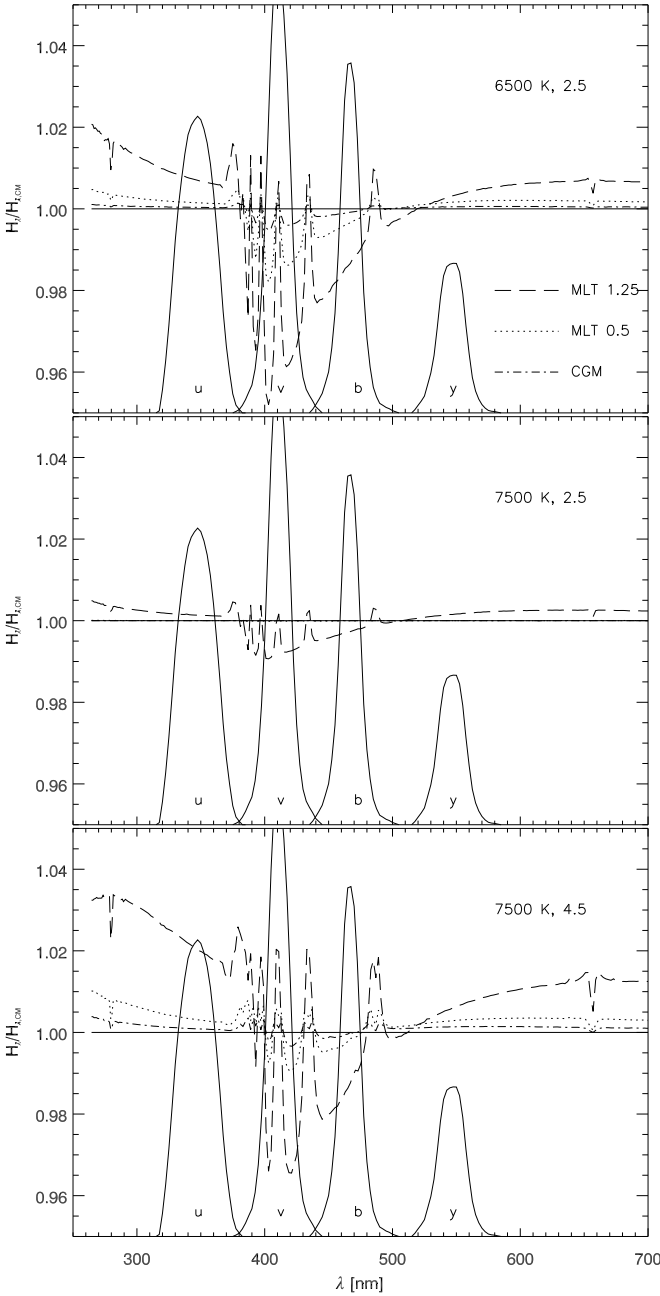


Fig. 9. Ratios of MLT and CGM to CM fluxes for three different combinations of T_{eff} and $\log g$. $[\text{M}/\text{H}]=-1$ for all cases. Relative transmissivity profiles of the Strömgren *uvby* filters are indicated (multiplied by a standard 1P21 photomultiplier response function).

Gardiner et al. (1999) reported a few opposite cases (see Sect. 2), but for parts of their sample of stars fundamentally known $\log g$ values were not available. An analysis of a larger sample of stars in binary systems with revised fundamental parameters for *both* $\log g$ and T_{eff} (Smalley et al. 2002) did not confirm the discrepancies previously found. Furthermore, for the case of F stars Smalley et al. (2002) noticed a larger systematic difference between fundamental effective temperatures and those obtained from H_{β} lines for MLT($\alpha=1.25$) than for less efficient con-

Table 2. Model parameters ordered according to increasing flux differences arising when using any two different convection models. The quantities listed in the columns labeled “blue”, “UV” and “red” are the maxima of $|H_{\lambda,\text{MLT1.25}}/H_{\lambda,\text{CM}} - 1|$ for the wavelength ranges 360–520 nm, 250–360 nm and 520–700 nm, respectively (cf. Fig. 9).

blue	T_{eff}	$\log g$	UV	red	T_{eff}	$\log g$
$[\text{M}/\text{H}] = +1$						
0.000	7500	2.5	0.000	0.000	7500	2.5
0.024	6500	4.5	0.011	0.005	6500	4.5
0.038	6500	2.5	0.012	0.007	6500	2.5
0.046	7500	4.5	0.022	0.011	7500	4.5
$[\text{M}/\text{H}] = 0$						
0.004	7500	2.5	0.003	0.001	7500	2.5
0.030	6500	4.5	0.014	0.007	6500	4.5
0.043	7500	4.5	0.022	0.008	6500	2.5
0.048	6500	2.5	0.027	0.013	7500	4.5
$[\text{M}/\text{H}] = -1$						
0.009	7500	2.5	0.006	0.003	7500	2.5
0.026	6500	4.5	0.023	0.007	6500	2.5
0.034	7500	4.5	0.030	0.011	6500	4.5
0.048	6500	2.5	0.034	0.015	7500	4.5

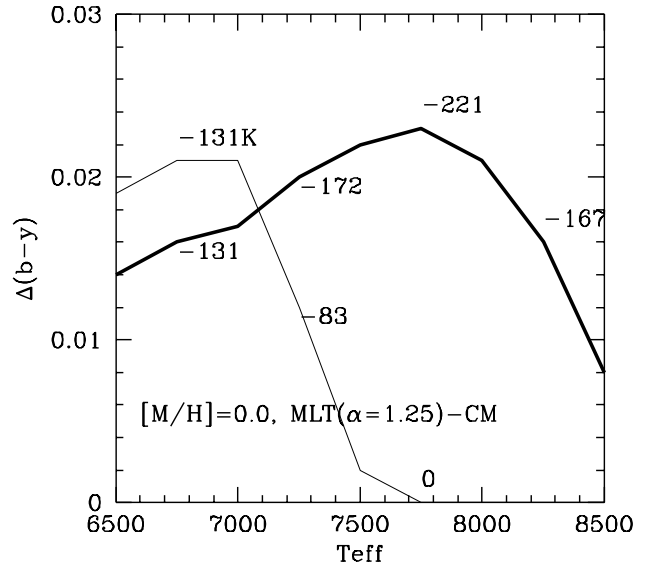


Fig. 10. Differences between $(b - y)$ indices computed using models differing only by the convection treatment. The thin line is for $\log g = 2.5$, the thick line for $\log g = 4.5$. For clarity, we indicate the temperature differences corresponding to the $(b - y)$ differences along the curves only for a few models.

vection models, although this discrepancy remains within the overall uncertainties.

Nevertheless, we have to emphasize that in models with deep convection zones (e.g. for Sun, Procyon) MLT($\alpha = 0.5$) and FST treatments have comparable effects on calculated fluxes, but not on atmosphere structure. They produce different temperature gradients in the deep layers, as can be seen in Figs. 2 and 3, but those cannot be distinguished by the computed BLPs. In

other words, the BLPs allow to discriminate among different values for the MLT parameter α , but not among MLT ($\alpha = 0.5$), CM, and CGM models. In any case, the sensitivity of BLPs to convection parameters depends significantly on the other physical parameters. This holds especially for the sensitivity to gravity change, which can be more important than usually expected.

In case of weakly efficient convection, fluxes and colors depend only weakly on the selected convection treatment. On the other hand, when the convection is highly efficient, then fluxes and colors become strongly dependent on the convection modelling, as the differences among the models show up more clearly within the photosphere. Thus, significant uncertainties on stellar global parameters arise from the convective treatment in model atmospheres. Ignoring these uncertainties can lead to systematic differences affecting subsequent interpretations.

The calculations of color and limb darkening partial derivatives are significantly improved when using the present model atmosphere grids which are finer spaced in T_{eff} and $\log g$ and have a higher resolution in the temperature distribution with depth (Barban et al. 2002). Smoothness of these derivatives is of crucial importance in the mode discrimination problem for non-radially pulsating stars, which is basically due to the dependence of the color amplitude ratios on these derivatives. Details of the required precision of these partial derivatives in order to be useful for mode identification will be given in Garrido et al. (2002). There we will show that the next space asteroseismology missions – COROT, MONS/Rømer and Eddington – will supply light curves with high enough precision to permit a direct comparison up to the second order to partial derivatives with respect to temperature and gravity as calculated with the present model atmospheres.

The improved resolution of the new model grids also avoids unphysical oscillations in evolutionary track calculations when using ATLAS9 model atmospheres as boundary conditions (see Sect. 4.1). Moreover, the possibility to choose among different convection models allows a self-consistent match between model atmospheres and model envelopes (Montalbán et al. 2001). However, we must stress here that the different relations T and $F_{\text{conv}}/F_{\text{tot}}$ vs. depth represent stars which are different in their radii and luminosities. The broad effects of the convective treatment can only be assessed by studying a complete stellar model, i.e. a model with an atmosphere and an internal structure which are consistently built with the same convection formulation. We will address this topic in follow up work (Kupka et al. 2002).

Acknowledgements. The authors would like to thank Gerard Thuillier for providing the SOLSPEC solar irradiance data. Many thanks go to Robert Kurucz for allowing us to use his model atmosphere code and opacity data. We would like to thank the referee, F. Castelli, for helpful comments and the rapid evaluation of the manuscript. This research was carried out within the working group *Asteroseismology-AMS*,

Table 3. Convergence criteria used for the Vienna grid computations.

	RMS	Maximum
primary		
ΔF_l	$\leq 1\%$	$\leq 5\%$
$\Delta F'_l$	$\leq 2\%$	$\leq 10\%$
		or $\leq 10\%$ ($N/10 \leq l \leq N$)
		and $\Delta T_l \leq 1\text{K}$ ($0 \leq l \leq N/10$)
secondary		
$\Delta F_l, \Delta F'_l$	$\leq 10\%$	$\leq 100\%$

supported by the Fonds zur Förderung der wissenschaftlichen Forschung (project *P13936-TEC*).

Appendix: Description of SMGT

The program can be run in either of two modes depending on the temperature structure used for initialization:

- In the *static* mode, an existing model file or a gray atmosphere is used.
- In the *dynamic* mode, an existing model file or a weighted average of all existing models within one grid step of each parameter is used. The weights are calculated in the following way: For each atmospheric parameter p , the quantity

$$\exp\left(-\frac{|p^i - p^m|}{p_{\text{max}} - p_{\text{min}}}\right) \quad (27)$$

is computed, where i denotes the initialization model, m the model to be computed, and $p_{\text{max/min}}$ the maximum and minimum of the parameter as given in the grid definition. The results for all parameters (at most four) are multiplied to yield the weight.

The state of convergence of a particular model is measured by calculating the RMS and the maximum of the flux errors (ΔF_l), the flux derivative errors ($\Delta F'_l$) and the temperature correction (ΔT_l) in all layers l . A model is considered as fully converged if these values satisfy certain criteria, which are given in Table 3 (labeled “primary”). Models for which these criteria cannot be achieved after a reasonable number of iterations are also stored, if they satisfy the criteria labeled “secondary” in Table 3, but the corresponding files are marked with “~”.

In order to achieve the convergence criteria without wasting time when no further improvements can be expected from further iterations, the required number of iterations is calculated and checked dynamically, after an initial sequence of 12 iterations. From a sequence of n iterations the ATLAS9 output is processed every $n/4$ iteration (but at least every 15th and at most every 3rd iteration) and the speed of convergence is characterized in the following way. The ratios between the rms errors of two subsequent iterations ($r_{F'}^i, r_{F'}^i$) are calculated. If they are found smaller than a threshold value (0.95), damping exponents are computed iteratively for the flux errors:

$$\gamma_F^i = [\gamma_F^{i-1} n^{i-1} - a \ln(1 - r_F^i)] / n^i, \quad (28)$$

where i goes from 2 to the number of processed outputs, γ_F^1 is set to zero or the value determined from the previous iteration sequence, $a = 1$ for $i = 2$ and $a = (n^i - n^{i-1})/n^i$ for $i > 2$, and an analogous formula is used for the flux derivative errors. The total number of iterations is then given by

$$n_{\text{tot}} = \text{int} \left(\frac{\ln(r_{\text{crit}})}{\ln(1 - \exp(-\gamma_F n))} \right)$$

$$\text{or } n_{\text{tot}} = \text{int} \left(\frac{\ln(r_{\text{crit}})}{\ln(r_F)} \right) \quad (29)$$

with

$$r_{\text{crit}} = \frac{\text{RMS}_{\text{prim}}(\Delta F_l)}{\text{RMS}(\Delta F_l)} \quad (30)$$

where the largest of the values resulting from ΔF_l or $\Delta F_l'$ is taken. Apart from the first iteration sequence, the actual number of further iterations is a fraction depending on the ratio between the current predicted number of total iterations and the previous prediction. The computations are terminated if the errors increase (after a few further trials) or if the total number of iterations would be too large (we use a limit of 480).

References

- Anders, E. & Grevesse, N. 1989, *Geochim. Cosmochim. Acta*, 53, 197
- Böhm-Vitense, E. 1958, *ZAp*, 46, 108
- Balona, L. A. & Evers, E. A. 1999, *MNRAS*, 302, 349
- Barban, C., Goupil, M. J., van 't Veer, C., et al. 2002, *A&A*, in preparation
- Barklem, P. S., Piskunov, N., & O'Mara, B. J. 2000, *A&A*, 363, 1091
- Biermann, L. 1948, *ZAp*, 25, 135
- Canuto, V. M. 1996, *ApJ*, 467, 385
- Canuto, V. M., Goldman, I., & Mazzitelli, I. 1996, *ApJ*, 473, 550
- Canuto, V. M. & Mazzitelli, I. 1991, *ApJ*, 370, 295
- . 1992, *ApJ*, 389, 724
- Castelli, F. 1996, in *ASP Conf. Ser. 108: Model Atmospheres and Spectrum Synthesis*, ed. S. J. Adelman, F. Kupka, & W. W. Weiss, 85
- Castelli, F. 1999, *A&A*, 346, 564
- Castelli, F., Gratton, R., & Kurucz, R. L. 1997, *A&A*, 318, 841, erratum: 1997, *A&A* 324, 432
- COROT web site. 2001, <http://www.astrsp-mrs.fr/projets/corot/pagecorot.html>
- Cox, J. P. & Giuli, R. T. 1968, *Principles of stellar structure* (New York, Gordon and Breach)
- D'Antona, F., Montalbán, J., Kupka, F., & Heiter, U. 2002, *ApJ*, 564, L93
- Fuhrmann, K., Axer, M., & Gehren, T. 1993, *A&A*, 271, 451
- Gardiner, R. B., Kupka, F., & Smalley, B. 1999, *A&A*, 347, 876
- Garrido, R. 2000, in *ASP Conf. Ser. 210: Delta Scuti and Related Stars*, ed. M. Breger & M. Montgomery, 67
- Garrido, R., Garcia-Lobo, E., & Rodriguez, E. 1990, *A&A*, 234, 262
- Garrido, R., Goupil, M. J., van 't Veer, C., et al. 2002, *A&A*, in preparation
- Gray, D. F. 1992, *The observation and analysis of stellar photospheres* (Cambridge University Press)
- Heiter, U., Kupka, F., Paunzen, E., Weiss, W. W., & Gelbmann, M. 1998, *A&A*, 335, 1009
- Hurlburt, N. E., Toomre, J., & Massaguer, J. M. 1986, *ApJ*, 311, 563
- Hurlburt, N. E., Toomre, J., Massaguer, J. M., & Zahn, J. 1994, *ApJ*, 421, 245
- Künzli, M., North, P., Kurucz, R. L., & Nicolet, B. 1997, *A&AS*, 122, 51
- Kupka, F. 1996, in *ASP Conf. Ser. 108: Model Atmospheres and Spectrum Synthesis*, ed. S. J. Adelman, F. Kupka, & W. W. Weiss, 73
- Kupka, F. 1999, *ApJ*, 526, L45
- Kupka, F. & Montgomery, M. H. 2002, *MNRAS*, 330, L6
- Kupka, F., Samadi, R., Lebreton, Y., et al. 2002, *A&A*, in preparation
- Kurucz, R. L. 1993, *CD-ROM 13*, SAO
- . 1998, <http://cfaku5.harvard.edu/>
- Lesieur, M. 1990, *Turbulence in fluids: stochastic and numerical modelling* (Dordrecht: Kluwer)
- Livingston, W., Donnelly, R. F., Grigor'ev, V., et al. 1991, in *Solar interior and atmosphere*, ed. A. N. Cox, W. C. Livingston, & M. S. Matthews (Tucson, AZ: University of Arizona Press), 1109
- Lockwood, G. W., Tueg, H., & White, N. M. 1992, *ApJ*, 390, 668
- Ludwig, H., Freytag, B., & Steffen, M. 1999, *A&A*, 346, 111
- Montalbán, J., Kupka, F., D'Antona, F., & Schmidt, W. 2001, *A&A*, 370, 982
- Morel, P., van 't Veer, C., Provost, J., et al. 1994, *A&A*, 286, 91
- Neckel, H. & Labs, D. 1984, *Sol. Phys.*, 90, 205
- Öpik, E. J. 1950, *MNRAS*, 110, 559
- Orszag, S. A. 1977, in *Fluid Dynamics, Les Houches Summer School of Theoretical Physics*, ed. R. Balian & J. L. Peube (New York: Gordon & Breach), 237
- Praskovskiy, A. & Oncley, S. 1994, *Physics of Fluids*, 6, 2886
- Schmidt, W. 1999, *Master's thesis*, Johannes Kepler University Linz, Austria
- Smalley, B., Gardiner, R. B., Kupka, F., & Bessell, M. S. 2002, *A&A*, in preparation
- Smalley, B. & Kupka, F. 1997, *A&A*, 328, 349
- Spiegel, E. A. 1957, *ApJ*, 126, 202
- Stein, R. F. & Nordlund, A. 1998, *ApJ*, 499, 914
- Stothers, R. B. & Chin, C. 1995, *ApJ*, 440, 297
- . 1997, *ApJ*, 478, L103
- Thuillier, G., Herse, M., Simon, P. C., et al. 1998, *Sol. Phys.*, 177, 41
- van 't Veer-Menneret, C., Bentolila, C., & Katz, D. 1998, *Contributions of the Astronomical Observatory Skalnaté Pleso*, 27, 223

- van 't Veer-Menneret, C. & Megessier, C. 1996, *A&A*, 309,
879, cited as VM
- Watson, R. D. 1988, *Ap&SS*, 140, 255